Time-Resolved Fluorescence Spectroscopy and Imaging of DNA Labeled with DAPI and Hoechst 33342 Using Three-Photon Excitation

Joseph R. Lakowicz,* Ignacy Gryczynski,* Henryk Malak,* Martin Schrader,# Peter Engelhardt,§ Hiroski Kano,¶ and Stefan W. Hell ¶

*Center for Fluorescence Spectroscopy and Medical Biotechnology Center, Department of Biochemistry and Molecular Biology, University of Maryland School of Medicine, Baltimore, Maryland 21201 USA; #Department of Medical Physics and Chemistry, University of Turku, FIN-20521 Turku, Finland; §Department of Virology, Haartman Institute, University of Helsinki, FIN-00014 Helsinki, Finland; and ¶Centre for Biotechnology, University of Turku, FIN-20521 Turku, Finland

ABSTRACT We examined the fluorescence spectral properties of the DNA stains DAPI (4′,6-diamidino-2-phenylindole, hydrochloride) and Hoechst 33342 (bis-benzimide, or 2,5′-bi-^{1}H-benzimidazole2′-(4-ethoxyphenyl)-5-(4-methyl-1-piperazinyl)) with two-photon ($2h\nu$) and three-photon ($3h\nu$) excitation using femtosecond pulses from a Ti:sapphire laser from 830 to 885 nm. The mode of excitation of DAPI bound to DNA changed from two-photon at 830 nm to three-photon at 885 nm. In contrast, Hoechst 33342 displayed only two-photon excitation from 830 to 885 nm. DAPI-DNA displayed the same emission spectra and decay times for $2h\nu$ and $3h\nu$ excitation. Hoechst 33342-DNA displayed the same intensity decay for excitation at 830 and 885 nm. Both probes displayed higher anisotropies for multiphoton excitation as compared to one-photon excitation with ultraviolet wavelengths, and DAPI-DNA displays a higher anisotropy for $3h\nu$ at 885 nm than for $2h\nu$ at 830 nm. We used 970-nm excitation of DAPI-stained chromosomes to obtain the first three-dimensional images with three-photon excitation. Three-photon excitation of DAPI-stained chromosomes at 970 nm was demonstrated by the power dependence in the fluorescence microscope.

INTRODUCTION

The increasing availability of intense laser sources with picosecond and femtosecond pulse widths has resulted in the increased use of two-photon excitation for time-resolved fluorescence and for fluorescence imaging microscopy. Two-photon excitation has been applied to a number of fluorophores, including proteins (Sammeth et al., 1990; Rehms and Callis, 1993; Lakowicz et al., 1992a, 1993, 1994a), DPH-labeled membranes (Lakowicz et al., 1992b), and stained DNA (Gryczynski and Lakowicz, 1994; Lakowicz and Gryczynski, 1992). Two-photon excitation seems to be especially useful in microscopic imaging, where the localized excited volume provides the equivalent of confocal imaging (Denk et al., 1990; Webb, 1990; Hell et al., 1994; Stelzer et al., 1994). Two-photon excitation has also been used to provide localized release of caged neurotransmitters and for studies of neuronal tissues (Denk, 1994; Denk et al., 1994). These biophysical uses of two-photon ($2h\nu$) excitation represent an extension of the pioneering uses of two-photon spectroscopy to study the excited-state symmetry of organic compounds (Wirth et al., 1981; Friedrich and McClain, 1980).

More recently we have found that use of the femtosecond pulses from Ti:sapphire lasers allows three-photon ($3h\nu$) excitation. In this process three long-wavelength photons are absorbed simultaneously to result in the lowest singlet excited state. Consequently, for molecules absorbing in the UV (300–350 nm), three-photon excitation can be accomplished using the fundamental output of a Ti:sapphire laser from 700 to 1000 nm. To date, three-photon excitation has been observed for tryptophan (Gryczynski et al., 1996a), DPH-labeled membranes (Malak et al., 1996), and the calcium-sensitive fluorophore Indo-1 (Gryczynski et al., 1995; Szmacinski et al., 1996). Before these studies, three-photon excitation has been reported only infrequently (Singh and Bradley, 1964; Pradere et al., 1966; Grubb et al., 1984), with greater attention given to the theory (Friedrich, 1981; Andrews and Ghoul, 1981; Cable and Albrecht, 1986). It was suggested that three-photon excitation could provide improved spatial resolution in microscopy (Singh and Bradley, 1964), and preliminary reports on this topic have already appeared (Hell et al., 1996; Webb, 1996).

In the present report we describe the fluorescence spectral properties of the DNA stain DAPI (4′,6-diamidino-2-phenylindole, hydrochloride) and Hoechst 33342 (HOE; bis-benzimide or 2,5′-bi-^{1}H-benzimidazole2′-(4-ethoxyphenyl)-5-(4-methyl-1-piperazinyl)) when excited with the fundamental output of a Ti:sapphire laser. Surprisingly, at wavelengths up to 885 nm, HOE displays only two-photon excitation, whereas DAPI displays three-photon excitation. Using DAPI-stained metaphase chromosomes from HeLa cells, we obtained 3D images of a chromosome with three-photon excitation of DAPI at 970 nm.

Received for publication 12 July 1996 and in final form 22 October 1996.

Address reprint requests to Dr. Joseph R. Lakowicz, Department of Biological Chemistry, University of Maryland School of Medicine, 108 N. Greene St., Baltimore, MD 21201-1503. Tel.: 410-706-7978; Fax: 410-706-8408; E-mail: jf@cfs.umbi.umd.edu (corresponding author for spectroscopy).

Reprint requests can also be addressed to Dr. Hiroski Kano and Dr. Stefan W. Hell, Centre for Biotechnology, University of Turku, P.O. Box 123, FIN-20521 Turku, Finland (corresponding authors for imaging).

0006-3495/97/02/567/12 $2.00

MATERIALS AND METHODS

DAPI and Hoechst 33342-labeled DNA

Calf thymus DNA was obtained from Sigma; DAPI and Hoechst 33342 were from Molecular Probes and were used without further purification. Samples were prepared in 10 mM Tris (pH 8). To minimize aggregation and increase solubility, the DNA was sonicated for 10 min in a sonicator bath and then centrifuged for 30 min at 10,000 rpm to sediment the particles.

The DNA concentration in base pairs was calculated using ϵ = 13,500 M^{-1} cm^{-1} at 259 nm. The concentration of DAPI and Hoechst 33342 were determined using ϵ = 33,000 M^{-1} cm^{-1} at 345 nm and ϵ = 42,000 m^{-1} cm^{-1} at 348 nm for the free forms of the probes, respectively. For studies with 2hν and 3hν of labeled DNA, the concentration in base pairs was 2.5 mM, and the extent of labeling was two probe molecules per 100 DNA base pairs.

Fluorescence spectroscopy

Multiphoton excitation was accomplished with the fundamental output of a Tsunami Ti:sapphire laser from Spectra Physics. The repetition rate of 80 MHz was held fixed by the Loc-to-Clock accessory. The repetition rate was divided by 8 by the Loc-to-Clock electronics and used as the 10-MHz reference signal for the frequency-domain (FD) instrument. The pulsewidth was near 80 fs. Its output (800–900 nm) was brought directly to the sample compartment and focused with a laser-quality lens (2 cm focal length). The emission was isolated with filters for intensity measurements and anisotropy decay. Intensity and intensity decay measurements were performed using magic angle conditions.

For emission spectra we used an SLM 8000 spectrofluorometer with a 10-nm bandpass. Solutions were in equilibrium with air. The signals from the DNA alone were less than 0.5% of that observed in the presence of DAPI or Hoechst 33342. For measurements of the dependence of the emission on laser intensity, the peak power was attenuated with neutral density filters. To avoid different widening the laser pulses by the neutral density filers, the same number of filters of the same design and thickness, but varying optical density, were used for the intensity measurements at various peak powers. All measurements were performed at room temperature near 20°C.

Frequency-domain intensity and anisotropy decays with multiphoton excitation were obtained on instrumentation described previously (Lakowicz and Gryczynski, 1991; Laczko et al., 1990). The intensity decay was assumed to be multiexponential:

$$I(t) = \sum_{i=1}^{n} \alpha_i e^{-t/\tau_i}, \tag{1}$$

where α_i are the preexponential factors, τ_i are the decay times, and n is the number of exponential components. The fractional intensity of each component in the steady-state emission is given by

$$f_i = \frac{\alpha_i \tau_i}{\sum_j \alpha_j \tau_i}. \tag{2}$$

In frequency-domain fluorometry, the sample is excited with an intensity-modulated light source, in the present case the output of a mode-locked Ti:sapphire laser or of a cavity-dumped dye laser. The phase angle (θ_ω) and the modulation (m_ω) of the emission are related to the intensity decay parameters, α_i and τ_i, and modulation frequency ω by

$$\phi_\omega = \arctan(N_\omega/D_\omega), \quad m_\omega = (N_\omega^2 + D_\omega^2)^{1/2}, \tag{3}$$

where

$$N_\omega = \frac{1}{J}\sum_{i=1}^{n} \frac{\omega\alpha_i\tau_i^2}{1+\omega^2\tau_i^2}, \quad D_\omega = \frac{1}{J}\sum_{i=1}^{n} \frac{\alpha_i\tau_i}{1+\omega^2\tau_i^2}, \quad J = \sum_{i=1}^{n} \alpha_i\tau_i. \tag{4}$$

The values α_i and τ_i are determined by minimization of the goodness-of-fit parameter

$$\chi_R^2 = \frac{1}{\nu}\sum_{\omega,k}\left(\frac{\phi_\omega - \phi_{\omega c}}{\delta\phi}\right)^2 + \frac{1}{\nu}\sum_{\omega,k}\left(\frac{m_\omega - m_{\omega c}}{\delta m}\right)^2, \tag{5}$$

where the subscript c indicates calculated values for known values of α_i and τ_i, $\delta\phi$ and δm the experimental uncertainties in the measured phase and modulation values, and ν is the number of degrees of freedom.

The hydrodynamics of DNA are complex, and interpretation of the anisotropy decay of labeled DNA requires the use of appropriate models (Schurr et al., 1992; Millar et al., 1982; Barkley and Zimm, 1979). However, the objective of the present report is not to advance on these elegant reports (Schurr et al., 1992; Millar et al., 1982; Barkley and Zimm, 1979), but rather to use the anisotropy decays to detect the effects of intense illumination on the solution conformation of DNA. Consequently, the frequency-domain anisotropy decays were analyzed in terms of the multicorrelation time model:

$$r_k(t) = \sum_j r_{jk}\, e^{-t/\theta_{jk}}, \tag{6}$$

where θ_j is the rotational correlation time displaying an amplitude r_j in the anisotropy decay. The subscript k indicates the mode of excitation (1hν, 2hν, or 3hν). In the absence of optical effects on DNA dynamics, we expect the correlation time (θ_j) to be independent of the mode of excitation. However, based on previous studies of DAPI (LakowiczandGryczynski, 1992) and Hoechst 33342 (Gryczynski and Lakowicz, 1994) with 1 hν and 2hν excitation, the amplitudes (r_{jk}) are expected to depend on the nature of the excitation process. The values of r_{jk} and θ_j are recovered by least-squares analysis of the differential polarized phase angles and modulated anisotropies (Lakowicz and Gryczynski, 1993), using an expression similar to Eq. 4. For the global analysis the same correlation times were used for each excitation wavelength (k), and the r_{jk} values we redistinct for each wavelength. The sum in Eq. 6 extends over the excitation wavelengths, where it is understood that phase and modulation data are available for two excitation wavelengths. The time 0 anisotropy is given by the sum of the amplitudes, $r_{ok} = \Sigma_j r_{jk}$.

Fluorescence anisotropy with multiphoton excitation

The time 0 anisotropy is a measure of the displacement of the emission transition moment from the direction of the polarized excitation. The theory for the expected r_{0k} values for two-photon excitation is complex (Callis, 1993; Chen and Van Der Meer, 1993; Wan and Johnson, 1994a,b), and analogous theories for 3hν excitation are not yet available. However, we have found that for many fluorophores the anisotropy behavior can be understood in terms of polarized photoselection with collinear transitions for the 2hν and 3hν transitions. In these cases the time 0 anisotropy is given by

$$r_{01}(\beta) = \frac{2}{5}\left(\frac{3}{2}\cos^2\beta_1 - \frac{1}{2}\right) \tag{7}$$

$$r_{02}(\beta) = \frac{4}{7}\left(\frac{3}{2}\cos^2\beta_2 - \frac{1}{2}\right) \tag{8}$$

$$r_{03}(\beta) = \frac{2}{3}\left(\frac{3}{2}\cos^2\beta_3 - \frac{1}{2}\right), \quad (9)$$

for $1h\nu$, $2h\nu$, and $3h\nu$ excitation, respectively. The factors 2/5, 4/7, and 2/3 originate with $\cos^2\theta$, $\cos^4\theta$, and $\cos^6\theta$ photoselection, where θ is the angle between the excitation polarization and the transition moment of the molecule. The angle β_k is the angular displacement between the absorption and emission transition, and need not be identical for each mode of excitation (k). More specifically, if the effective β's for one-, two-, and three-photon excitation are identical, then the time 0 anisotropies will be related by Eqs. 7–9. However, fluorophores can display more complex behavior, as has already been observed for tryptophan derivatives and proteins (Lakowicz et al., 1992a; Lakowicz and Gryczynski, 1993; Callis, 1993).

For one-, two-, and three-photon excitation the maximum anisotropies for $\beta_k = 0°$ are 0.40, 0.571, and 0.667, respectively. Observation of a larger anisotropy for three- versus two-photon excitation provides strong evidence for three-photon excitation. We note that the above description is somewhat simplified, and that multiphoton transitions are more correctly described as tensors (Callis, 1993; Chen and Van Der Meer, 1993; Wan and Johnson, 1994a,b). For the present data the simple theory described in Eqs. 7–9 is adequate for interpretation of the results.

DAPI staining of human metaphase chromosomes isolated from HeLa cells

Cells in metaphase were collected by shaking from cultured HeLa cells after incubation (12–48 h) in colchicine according to conventional cytogenetical methods. Briefly, chromosomes were isolated after (15 min) hypotony in 75 mM KCl, collected by centrifugation, and washed (2×) with (60%) acetic acid and kept in (60%) acetic acid (at −20°C) until use. A small amount (3–5 μl of a loose pellet) of metaphase chromosomes was applied (1–2 min) on a coverglass, washed (1–2×) with (60%) acetic acid and (3–4×) HM (40 mM HEPES, pH 7.4, 5 mM $MgCl_2$) buffer solution, stained (30 min) with DAPI (0.5 = μg/ml) in HM, washed with HM and mounted, under another coverglass, in buffered glycerol solution (90% glycerol (Merck, fluorescence free) 40 mM HEPES (Sigma), pH 7.4, and 5 mM $MgCl_2$, with 10–20 mM 2-mercaptoethanol included as an antifading substance). Preparations were kept at −20°C until use.

Chromosomal imaging

The experiments were carried out with a stage scanning fluorescence microscope capable of scanning the sample with a precision of 10 nm in three dimensions (Hell et al., 1995) (Melles Griot, Cambridge, England). The illumination light was focused into the specimen by a high-numerical-aperture lens (Leitz Planapo, 100×, 1.4, oil). The fluorescence light was collected by the same lens and directed toward a pinhole. The opening of the pinhole was about 5 times larger than the back-projected Airy disk, so that the microscope was not confocalized and the potential axial discrimination was minimized. The role of the pinhole rather was the rejection of ambient light. The light passing through the pinhole was focused onto the sensitive area of an avalanche photodiode (EG&G SPCM-AQ-131) operating in the photon counting mode. The fluorescence light was separated from the illumination light by a suitable dichroic bandpass transmitting between 410–500 nm and a 2-mm-thick stack of blue-colored glass BG39 (Schott, Inc.). We used the light of a mode-locked Ti:sapphire laser (Coherent, Mira 900 F) providing a train of about subpicosecond pulses with a duration of about 140 fs in the focal region of the lens (Hanninen and Hell, 1994).

The original confocal raw data volumes of the DAPI-stained metaphase chromosomes were converted to bytes, inverted, y and z flipped, and z-direction interpolated (2×), when it was considered necessary to get isometric pixel sizes in all directions.

High-quality animations of the confocal volumes (around the x or y axis) in jpeg format, with (or without) additional interpolation (3×) in all (x, y, z) directions, including light settings, were produced with the volume-render program FUNCS, with options for α blending, on a Silicon Graphics computer. The jpeg-formatted animations were visualized in stereo (liquid stereo-glasses for a Silicon Graphics computer) with the program JPEGANIM. The animations were further converted to pict format for mono- or stereo-inspection as red-green (blue) composite pictures to be visualized with the program National Institutes of Health-image in Macintosh computers.

RESULTS

Emission spectra and mode of excitation of DAPI or Hoechst 33342-labeled DNA

Emission spectra are shown in Fig. 1 for DAPI-DNA for excitation at 360, 830, and 885 nm. The emission spectra are essentially equivalent, irrespective of the excitation wavelength. We examined the nature of the long-wavelength excitation by attenuating the peak laser power using neutral density filters. A twofold attenuation of the incident light for 360-nm excitation results in a twofold attenuation of the emission (Fig. 1). For 830-nm excitation a twofold attenuation results in a fourfold decrease in the DAPI emission. At 885-nm excitation a twofold decrease in the incident intensity results in an eightfold decrease in the signal from DAPI. This dependence on the square and cube of the laser power suggests that the emission is due to two- and three-photon excitation, at 830 and 885 nm, respectively.

We were surprised by the observation of DAPI emission at these long excitation wavelengths and examined the dependence on laser power in more detail. Two-photon excitation of DAPI at 885 nm seemed unlikely because the one-photon absorption spectra do not display significant absorbance above 420 nm (Fig. 4, below), and thus one does not expect two-photon excitation at 885 nm. To determine the nature of the long-wavelength excitation we examined the dependence of the emission intensity on the incident laser power (Fig. 2). These data show that the observed

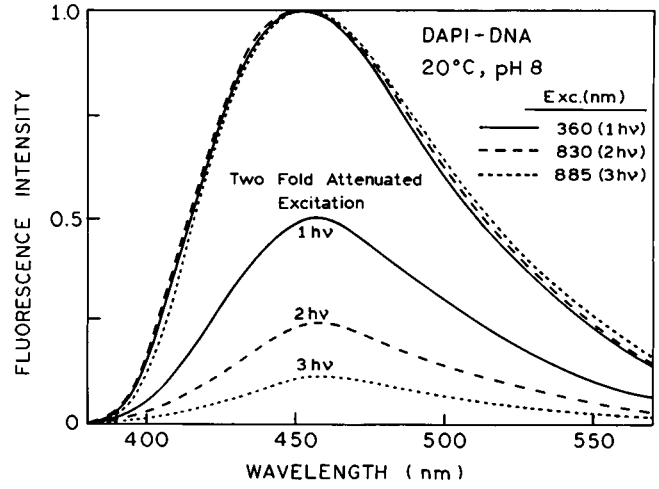

FIGURE 1 Normalized emission spectra of DAPI-DNA for excitation at 360, 830, and 885 nm. Also shown are the emission spectra with a twofold attenuation of the excitation.

intensity of DAPI-DNA is proportional to the cube of the laser power at 885 nm, and to the square of the laser power at 830 nm.

We also examined the emission spectra of HOE-DNA for 830 and 885 nm excitation. The emission spectra were essentially equivalent for excitation in the UV (360 nm) or for long wavelength excitation (not shown). However, we were surprised to observe that the mode of HOE-DNA excitation remained a two-photon process, even at 885 nm (Fig. 3). This observation illustrated the importance of detailed spectroscopic studies of a fluorophore before its use in multiphoton microscopy. Based on the absorption spectra of these samples (Fig. 4), it is not obvious to us that at 885 nm DAPI and Hoechst 33342 would display $3h\nu$ and $2h\nu$ excitation, respectively, particularly because DAPI displays a longer wavelength one-photon absorbance.

In more recent studies (Gryczynski et al., 1996b) we examined the effect of wavelength on the mode of excitation in more detail. We found that Hoechst 33342-DNA displays a mixture of $2h\nu$ and $3h\nu$ up to 910 nm (Gryczynski et al., 1996b). A preliminary report has suggested that Hoechst 33342 displays $3h\nu$ at 1047 nm (Wokosin et al., 1996), but the conclusion is stated to be speculative. Hence it appears that Hoechst 33342 can display $3h\nu$, but this requires wavelengths longer than 910 nm.

Intensity and anisotropy decays of DAPI and Hoechst 33342-labeled DNA

The intensity and especially the anisotropy decays are known to be sensitive indicators of the conformation and dynamics of biological molecules. In principle, photobleaching is not expected to result in changes in decay time, because the fluorophores are no longer fluorescent. However, we have noticed that other fluorophores, in particular a calcium probe (Lakowicz et al., 1994b), display lifetime changes with intense illumination, which we interpret as phototransformation of the probes. Hence the intensity decay can be an indicator of undesired photo effects on macromolecules.

We examined these time-resolved decays with long wavelength excitation. We reasoned that detrimental effects of the intense long wavelength illumination would be revealed by changes in the decay times or correlation times. These data could thus determine whether imaging of macromolecules would be possible without unacceptable photo effects. Frequency-domain intensity decay of DAPI-DNA is shown in Fig. 5 for $2h\nu$ and $3h\nu$ excitation. The intensity

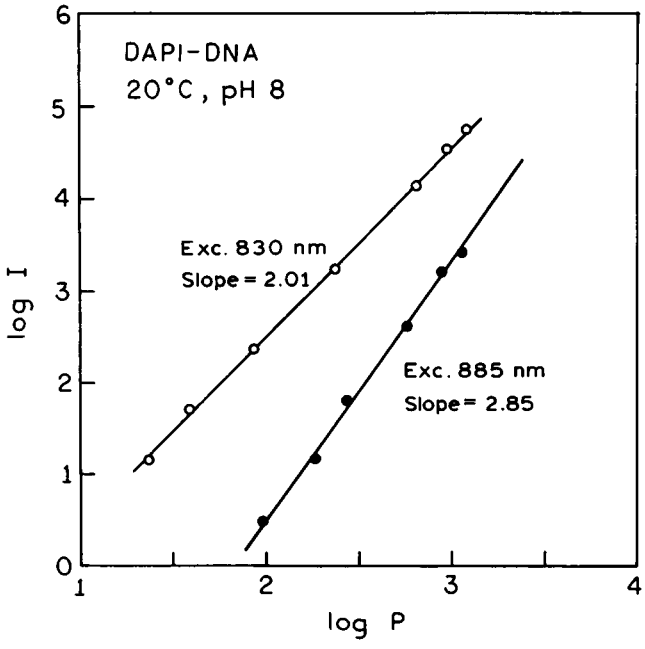

FIGURE 2 Dependence of the emission intensity of DAPI-DNA on incident power at 830 and 885 nm. The power is in milliwatts.

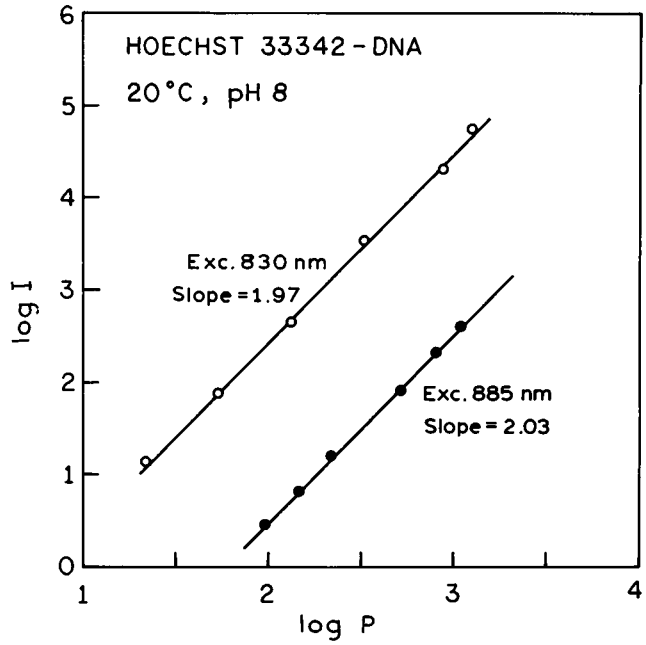

FIGURE 3 Dependence of the emission intensity of Hoechst 33342-DNA on incident power at 830 and 885 nm. The power is in milliwatts.

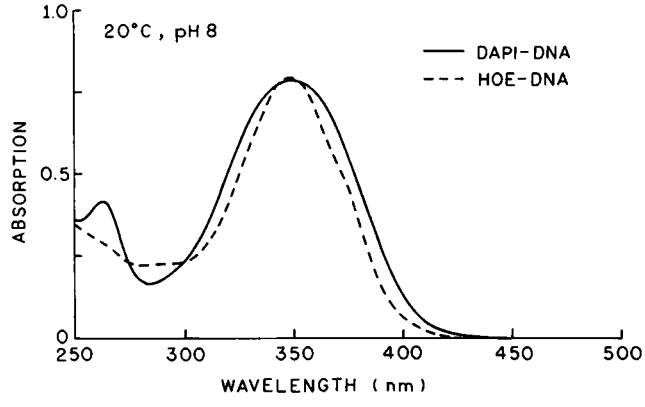

FIGURE 4 Absorption spectra of DAPI-DNA and Hoechst 33342-DNA.

decay parameters are essentially the same for 2hν and 3hν excitation (Table 1) and are similar to those observed previously for 1hν at 360 nm (Table 1). Similar results were obtained for HOE-DNA (Table 2), wherein the intensity decays were independent of the excitation wavelength.

We also performed a global analysis of the intensity decays of DAPI-labeled (Table 1) and HOE-labeled (Table 2) DNA using the data for both excitation wavelengths. Global analysis of the data at two excitation wavelengths provides a sensitive indicator of the sameness or difference of the intensity decays because the data at two wavelengths are fit to the same decay parameters. The global analysis results in the same intensity decay as for the individual analyses, and the value of χ^2_R was not elevated. These results demonstrate that the intensity decay was not altered by the mode of excitation and suggest that DNA is not disrupted by the moderately intense illumination required for three-photon excitation.

Anisotropy decays of DAPI-DNA and HOE-DNA is shown in Figs. 6 and 7, respectively. For both labeled DNAs the same correlation times were recovered for all excitation wavelengths (Tables 3 and 4). In the case of DAPI-DNA the FD anisotropy data are distinct for 2hν and 3hν at 830 and 885 nm, respectively. The differential phase angles and modulated anisotropies are larger for the longer excitation wavelengths, which is consistent with the higher level of photoselection for fluorophores with 3hν versus 2hν excitation (Eqs. 7–9). For HOE-DNA the FD anisotropy data are equivalent for both excitation wavelengths (Fig. 7), as expected for the same 2hν excitation at both wavelengths (Fig. 3). As for the intensity decays, the correlation times are similar to those observed previously for 1hν at 360 or 380 nm (Tables 3 and 4). The time 0 anisotropy is larger for 2hν and 3hν than for 1hν of DAPI (Table 3) or Hoechst 33342 (Table 4). Importantly, it was possible to globally fit the FD anisotropy data to the same correlation times for 830 and 885 nm excitation (Tables 3 and 4). These results suggest that the DNA molecules do not suffer adverse effects on significant heating when used with multiphoton excitation at commonly available Ti:sapphire wavelengths, thus enabling multiphoton imaging.

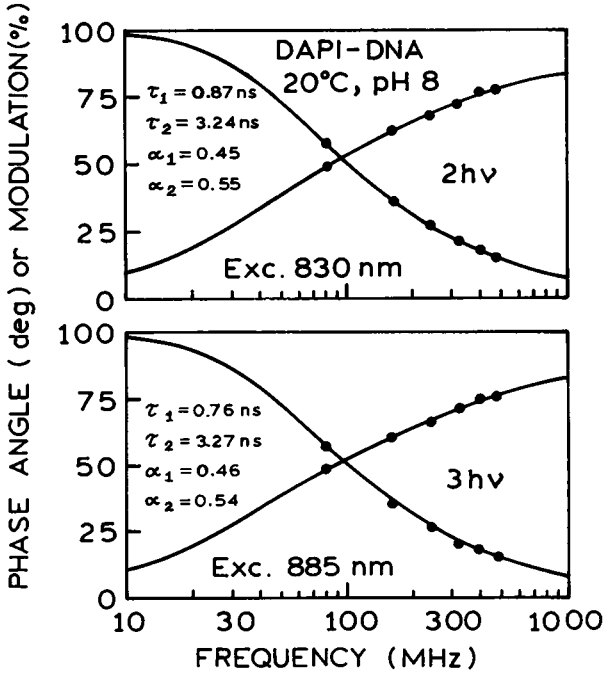

FIGURE 5 Frequency-domain intensity decay of DAPI-DNA with 2hν and 3hν excitation.

TABLE 1 Multiexponential intensity decay analysis of the DAPI-DNA fluorescence with multiphoton excitation

Excitation wavelength	τ_i (ns)	$\bar{\tau}$ (ns)	α_i	f_i	χ^2_R
830 nm, 2hν	0.87		0.45	0.18	
	3.24	2.82	0.55	0.82	2.1*
885 nm, 3hν	0.76		0.46	0.17	
	3.27	2.84	0.54	0.83	2.0
830 and 885 nm# (global)	0.81		0.455	0.17	
	3.25	2.84	0.545	0.83	4.1
360 n, 1hν†	1.25		0.35	0.15	
	3.93	3.53	0.65	0.85	2.1

*The values of χ^2_R were calculated using $\delta\theta = 0.3°$ and $\delta m = 0.007$.
#The decay times and amplitudes were global parameters.
†Lakowicz and Gryczynski, 1992.

Anisotropy and the mode of excitation

We examined the dependence of the anisotropy on incident power. For DAPI (Fig. 8) the anisotropy is different for excitation at 830 and 885 nm, but each value is independent of laser power over a wide range of power. This suggests that at these wavelengths one can be reasonably certain of the mode of excitation. At an intermediate wavelength of

TABLE 2 Multiexponential intensity decay analysis of the Hoechst 33342-DNA fluorescence with multiphoton excitation*

Excitation wavelength	τ_i (ns)	$\bar{\tau}$ (ns)	α_i	f_i	χ^2_R
830 nm, 2hν	1.33		0.52	0.32	
	3.02	2.49	0.48	0.68	2.3
885 nm, 2hν	1.41		0.51	0.33	
	3.23	2.62	0.49	0.67	2.8
830 and 885 nm (global)	1.40		0.52	0.32	
	3.11	2.56	0.48	0.68	2.5
380 nm, 1hν#	2.13		0.80	0.70	
	3.61	2.57	0.20	0.30	2.2

*See Table 1.
#Gryczynski and Lakowicz, 1994.

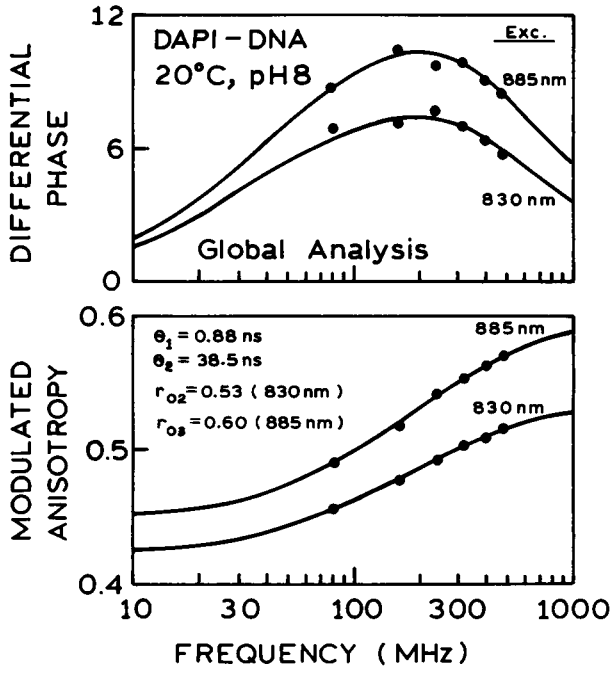

FIGURE 6 Frequency-domain anisotropy decays of DAPI-DNA with 2hν (830 nm) and 3hν (885 nm) excitation.

860 nm the anisotropy of DAPI-DNA depends on laser power (Fig. 8). This suggests that the mode of excitation is changing from 2hν to 3hν as the power is increased. In the case of HOE-DNA the same anisotropy was observed for 830, 860, and 885 nm excitation (Fig. 8), indicating that the excitation remains a two-photon process at these wavelengths over a range of power levels. Because the anisotropy is independent of fluorescence intensity, anisotropy measurements are recommended for clarifying the mode of excitation in multiphoton microscopy. Furthermore, the anisotropy of a known compound can be used to estimate the intensity at the focal point of the microscope.

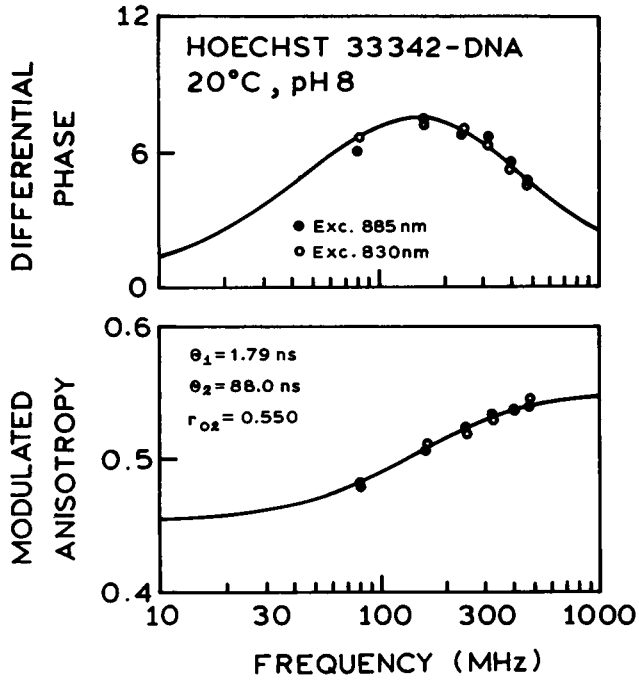

FIGURE 7 Frequency-domain anisotropy decay of DNA-Hoechst 33342-DNA for excitation at 830 and 885 nm.

TABLE 3 Multicorrelation time analysis of the DAPI-DNA complex

Excitation wavelength	θ_j (ns)	r_j	r_o	χ^2_R
830 nm, 2hν	0.79	0.10		
	26.9	0.43	0.53	0.9*
885 nm, 3hν	0.92	0.16		
	55.3	0.44	0.60	4.0
830 and 885 nm (global)	0.88	0.11 and 0.16#		
	38.5	0.42 and 0.44	0.60	2.6
360 nm, 1hν†	1.59	0.062		
	93.9	0.28	0.34	1.3

*The value of χ^2_R was calculated using $\delta\Delta = 0.3°$ and $\delta\Lambda = 0.007$.
#The correlation times were global parameters; the anisotropy amplitudes were nonglobal.
†Lakowicz and Gryczynski, 1992.

Spatial resolution with multiphoton excitation

In a previous report we suggested that the cubic intensity dependence of 3hν excitation could result in improved spatial resolution in microscopy (Gryczynski et al., 1995). This feature of multiphoton excitation is illustrated in Fig. 9, where we compare the size of the excited volume for 2hν and 3hν excitation. We examined the spatial distribution of the excited fluorophores by observation with an optical fiber positioned on a 50-μ vertical slit, 3 mm high (Fig. 9), as described previously (Gryczynski et al., 1995).

TABLE 4 Multicorrelation time analysis of the Hoechst 33342-DNA complex*

Excitation wavelength	θ_j (ns)	r_j	r_o	χ^2_R
830 nm, 2hν	1.66	0.15		
	89.4	0.39	0.54	1.1
885 nm, 2hν	1.79	0.15		
	88.0	0.40	0.55	3.2
830 and 885 nm (global)	1.75	0.15		
	89.1	0.40	0.55	3.0
380 nm, 1hν#	1.4	0.07		
	85.8	0.31	0.38	1.0

*See Table 3.
#Gryczynski and Lakowicz, 1994.

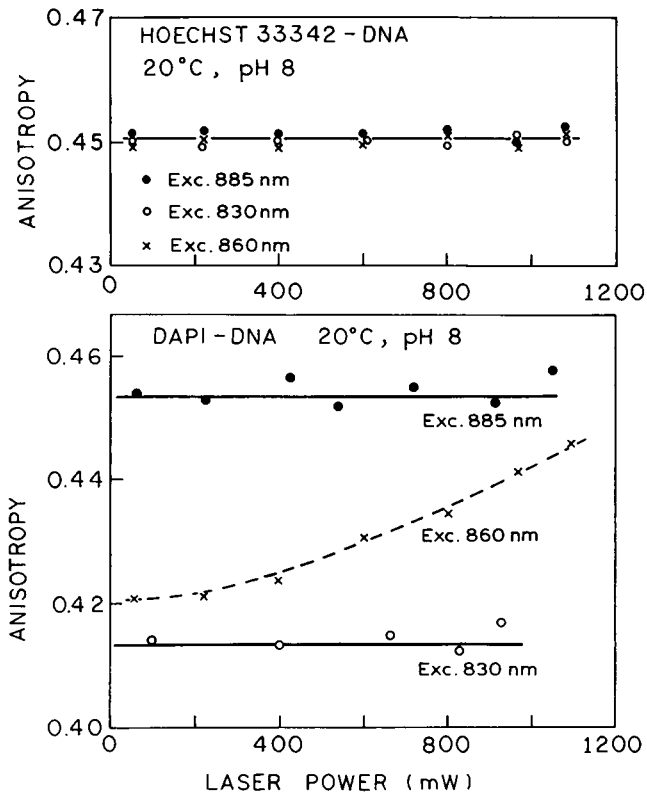

FIGURE 8 Dependence of the steady-state anisotropy of DAPI-DNA and HOE-DNA on incident power at 830, 860, and 885 nm.

Similar spatial distributions were observed for DAPI-DNA with 830-nm excitation and for HOE-DNA with 885-nm excitation (Fig. 9, *left*), which is consistent with two-photon excitation of both probes. In contrast, a smaller excited volume was observed for 3hν of DAPI-DNA with 885-nm excitation, which is most probably the result of the cubic three-photon process. Improved spatial resolution with 3hν excitation was also shown previously with the scintillator 2,5-bis(4-biphenyl)oxazole (Hell et al., 1996).

Three-photon chromosome imaging

To demonstrate the practical application of three-photon imaging, we chose to examine metaphase chromosomes isolated from HeLa cells and stained with DAPI. As shown in Fig. 2, the fluorescence intensity of DAPI with 3hν excitation is about 100-fold lower than that of two-photon excited DAPI. In 3hν microscopy, the major challenge is the efficient generation and collection of fluorescence photons. The latter determines the signal-to-noise ratio (SNR) in the image and therefore the reliability with which the information can be retrieved from the specimen. The cubic dependence of 3hν excited fluorescence leads to a strong suppression of otherwise noticeable contributions from the outer region of the focus. The suppression results in the formation of a spatially well-confined focal volume that is mathematically described by a three-dimensional effective point spread function (E-PSF). For a typical excitation wavelength of 900 nm and a numerical aperture of 1.4 (oil), the typical extent of the E-PSF is about 0.2 μm and 0.6 μm in the lateral and axial directions, respectively (Hell et al., 1996). The typical volume is 50–100 attoliters, which is about 7 orders of magnitude smaller than in the spectrometric arrangement of Figs. 1–8. On the other hand, in high-aperture microscopy, the total collection angle is larger by about two orders of magnitude. When focusing into a uniform solution of fluorophores, the fluorescence signal is about 5 orders of magnitude weaker in a microscope than in a spectrometer. Hence the practical realization of 3hν microscopy is a challenging endeavor.

A simple yet useful strategy for investigating the applicability of 3hν excitation in microscopy is to raise the illumination intensity to the highest level that the samples can withstand without showing any sign of degradation. The use of pulsed illumination reduces the total thermal load of the sample, but high peak intensities increase the risk of a dielectric breakdown of the material. A possible outcome of a 3hν excitation experiment in a microscope could have been that the required intensities are above the dielectric breakdown threshold. However, initial experiments by us (Hell et al., 1995) and others (Webb, 1996; Wokosin et al., 1996) have shown this not to be the case. In our experiments (Hell et al., 1996) we have demonstrated the two key features of 3hν excitation microscopy, namely the cubic dependence of the fluorescence on the power of the excitation light and the axial superresolution. In the following, we show that it is possible to perform 3hν microscopic imaging of biological specimens with DAPI-labeled human metaphase chromosomes at excitation wavelengths near 970 nm, which is beyond the threshold for three-photon excitation. We confirmed the three-photon nature of excitation of DAPI at this wavelength by measuring the fluorescence signal in the microscope as a function of the excitation power.

Fig. 10 shows an *XY* image of a DAPI-labeled metaphase chromosome extracted from a HeLa cell recorded at 970 nm. The pixel size of the image is 35 nm in the x and y directions. The pixel dwell time is 2 ms, and the total time for one image was 70 s, including the scanning dead time. The average power of the incident light was 3.4 mW, which amounts to an estimated peak intensity of about 80 GW/cm^2. At this intensity, we obtained about 10 photons per pixel for those sites of the chromosome where the label was strongest. The profile in Fig. 10 shows the raw data along the marked line.

To determine the dependence of the observed signal on the excitation power, we recorded a series of *XY* images of the same chromosome at different excitation powers. Fig. 11 *a* shows the signal in the images as a function of the average power. The series is a round-trip measurement starting with a low average power of 0.8 mW. We recorded *XY* images of the same specimen site with increasing intensity and then continued the series by returning to the low

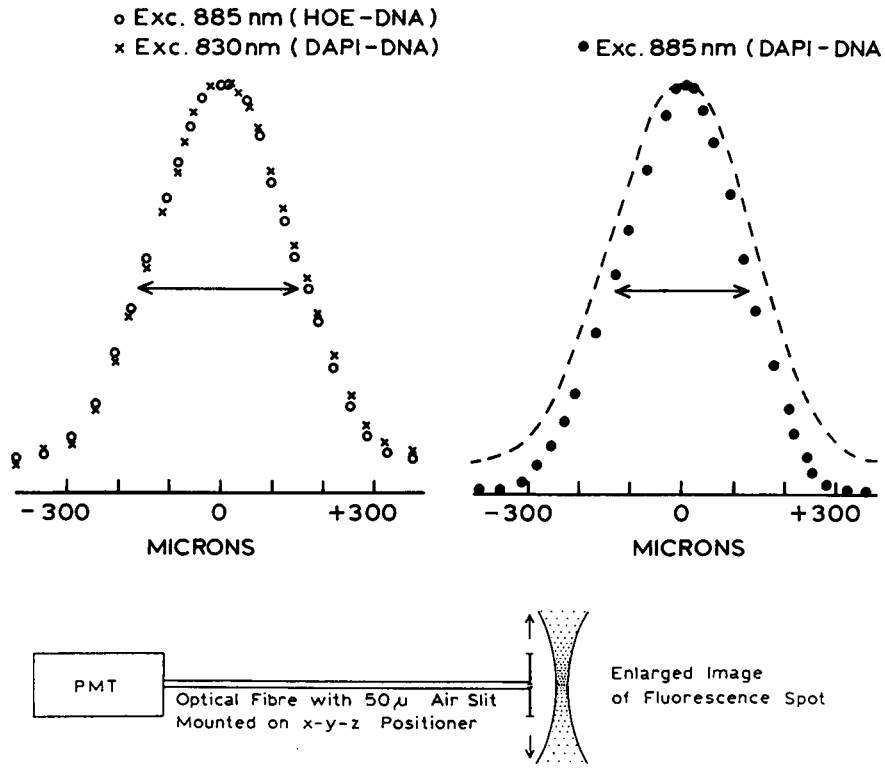

FIGURE 9 Spatial distribution of fluorescence for 2hν and 3hν excitation of DAPI-DNA and Hoechst 33342-DNA.

excitation power. In Fig. 11 *a* we find a slope larger than 2.5, thus revealing that a third-order process is involved in the fluorescence signal. Fig. 11 *b* shows a similar round-trip measurement for DAPI dissolved in glycerol in the microscope. For this purpose we dissolved DAPI (Molecular Probes) in glycerol and placed a drop between two coverslips. The measurements of Fig. 11 *b* were carried out at the same numerical aperture (oil immersion 1.35) and wavelength (970 nm) as the chromosome images and differ from the spectroscopic data by the fact that the fluorescence molecules could not be exchanged by stirring. The double-logarithmic plot reveals a power dependence of 2.95, thus clearly demonstrating the three-photon nature of excitation.

Importantly, the intrinsic confocal capability also allows three-dimensional imaging of the chromosome by recording a whole 3D data stack. A complete three-photon 3D stack is shown in Fig. 12. The data stack consists of 50 independent lateral *xy* images that are axially separated by 80 nm. The stack has been processed with an image-processing algorithm that interpolated between the pixel and provided a volume rendering of the object (Engelhardt et al., 1994). As a result, the voxels with high intensity appear denser. We found 8–10 mW average power to be the upper limit at which microscopy could be performed in our sample. Yet Fig. 12 shows that this is sufficient to image the structure of the chromosome with 3hν excitation with great detail.

DISCUSSION

In recent years we have observed the increased experimental possibilities resulting from high repetition rate dye lasers. This trend has continued with the introduction of mode-locked Ti:sapphire lasers, which are simpler to operate than dye lasers and provide shorter pulsewidths near 100 fs. However, the fundamental output of the Ti:sapphire lasers is at maximum from 800 to 900 nm, which is too long for the excitation of many biochemical fluorophores.

The use of Ti:sapphire lasers with two-photon excitation is currently limited by their long wavelengths, resulting in attempts to obtain wavelengths below 700 nm from these lasers (Spectra Physics Lasers, 1995). The use of three-photon excitation may allow the use of Ti:sapphire lasers at their most efficient wavelengths near 800 nm. However, we did not know whether the biochemical samples would undergo excessive heating or dielectric breakdown upon illumination at these wavelengths and intensities. The similar anisotropy decay of DAPI-DNA with two- and three-photon excitation argues against significant heating of the sample. In other experiments we have observed similar correlation times for Indo-1 with one- and three-photon excitation (Szmacinski et al., 1996), and the same phase transition temperature for bilayers labeled with 1,6-diphenyl-hexatriene and studies by three-photon excitation (Malak et al., 1996). In this report we have shown that 3hν excitation of DAPI-labeled DNA could be accomplished without changes in the intensity or anisotropy decays, suggesting the absence of structural perturbations with the locally intense excitation. This favorable outcome is probably due to the fact that these wavelengths are near the region of minimum water absorption (Svoboda and Block, 1994; Denk et al., 1995). In totality, these results suggest that three-photon

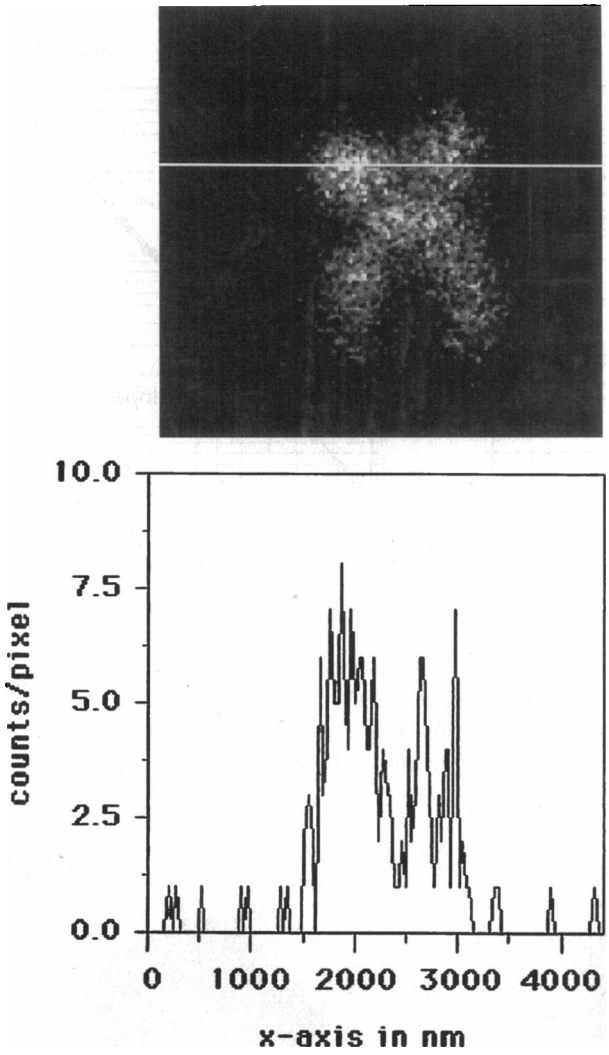

FIGURE 10 Two-dimensional image of a HeLa cell metaphase chromosome with 3hν excitation of DAPI at 920 nm. This is one of 50 images used for the 3D reconstruction (Fig. 12) at 970 nm. The profile shows the raw intensity data (counts) along the marked line across the chromosome image.

excitation of biomolecules is practical with present laser technology.

It is interesting to speculate on the origin of the long wavelength two-photon excitation of Hoechst 33342 at 885 nm. Examination of the absorption spectra in Fig. 4 would cause one to predict that the mode of excitation would change from 2hν to 3hν for Hoechst 33342 at shorter wavelengths than for DAPI. However, the opposite was observed, and Hoechst 33342 still displays 2hν excitation at 885 nm. This suggests the presence of an allowed two-photon transition near 450 nm, which is not visible in the absorption spectra of Hoechst 33342. Such a result is analogous to that found for polyenes, which are known to display allowed two-photon transitions at lower energies than the lowest energy one-photon transitions (Hudson and Kohler, 1974; Fang et al., 1978). For instance, 1,6-diphenylhexatriene (DPH) displays a maximum in its two-photon absorption spectra near 400 (800) nm, considerably longer than the lowest one-photon transition near 385 nm (Svoboda and Block, 1994). Hence it appears that Hoechst 33342 has energy levels and transitions comparable to those of polyenes, whereas DAPI does not display such a lower energy two-photon transition. This is surprising, given the structural similarity of DAPI and Hoechst 33342 to both containing phenyl-indole groups. These results suggest that one cannot readily predict the 2hν and 3hν spectral properties of fluorophores from the one-photon spectra.

In the second part of the manuscript we demonstrated fluorescence imaging at high resolution with three-photon excitation. We showed that at an excitation wavelength of around 970 nm, the chromosome fluorescence image was dominated by a third-order excitation process. One can notice that the power dependence does not follow an exact cubic law, as one might expect for ideal three-photon imaging. We suggest two reasons for these deviations, one of them being a weak but measurable second-order autoluminescence from the sample that we could also record from unstained chromosomes. As stirring is not possible in a microscope, other effects such as photobleaching cannot always be avoided. Apparently photobleaching played a role in the power dependence measurement in Fig. 11 *a* or other effects that are intrinsic to the chromosome sample. We also recorded images where the difference between the increasing and decreasing measurement subseries was less pronounced. In Fig. 11 *b*, which shows the DAPI-glycerol counterpart to Fig. 11 *a*, an impressive third-order power dependence is found. Whereas the fluorescence from the DAPI-glycerol solution in the microscope was governed by a cubic power law, we were not able to completely establish a cubic law on the glycerol-embedded DAPI-chromosome in the 890–940 nm range; rather the slope was close to 2. This does not exclude a three-photon nature of excitation, but it appears that effects due to the sample play a role, and it seems also that the precise localization of the two- to three-photon transition on a labeled biological sample can be challenging in multiphoton microscopic imaging.

With a wavelength of around 970 nm and probably higher, one can image DAPI-labeled chromosomes by three-photon excitation. As we have demonstrated elsewhere (Hell et al., 1996), the three-photon excitation point spread function is spatially narrower than its two-photon excitation counterpart, as long as one uses the same wavelength of excitation. The generally weaker signal of three-photon fluorescence can compromise the full benefit of the increased resolution, but an obvious benefit of three-photon excitation in the near infrared is the possibility of performing both two- and three-photon excitation images at the same wavelength by using multilabeled specimens. An example for this is a cell featuring a DAPI-labeled nucleus and rhodamine or fluorescein isothiocyanate-labeled cell organelles. A further advantage of 3hν excitation is the possibility of extending the excitation to the deep UV for proteins (Gryczynski et al., 1996a). In this case, the wave-

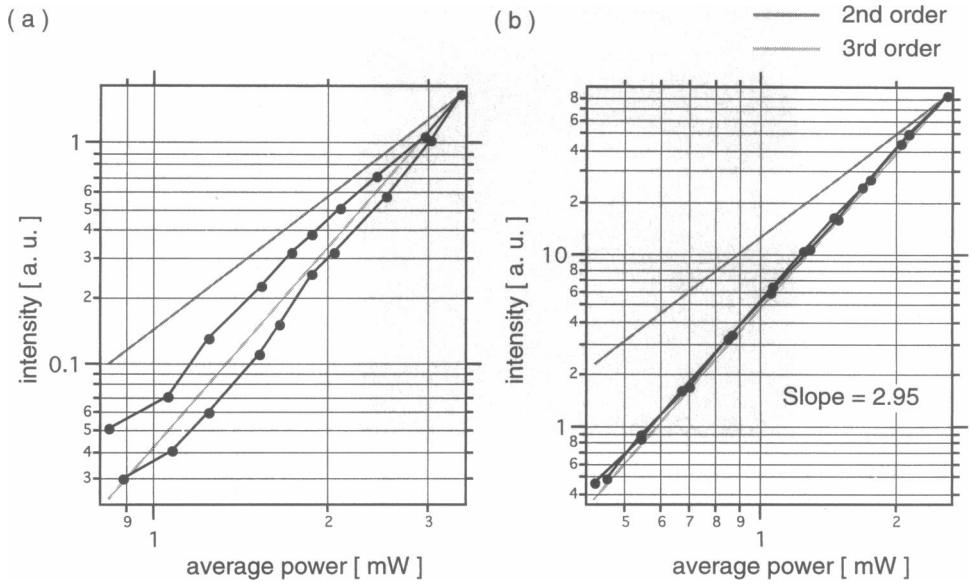

FIGURE 11 Fluorescence as a function of excitation power measured (*a*) on the imaged chromosome and (*b*) in a solution of DAPI dissolved in glycerol in a high-aperture microscope at 970-nm excitation.

length of the fluorescence light may be shorter, so that the poor transmissivity of the lenses and other optics should be considered. This problem can be alleviated by placing the detector immediately below the sample. A further interesting application is three-photon excitation 4Pi-confocal microscopy (Hell et al., 1995). The latter is predicted to feature a sharp focus consisting of a single peak that is about 200 nm in the lateral and 150 nm in the axial direction. In

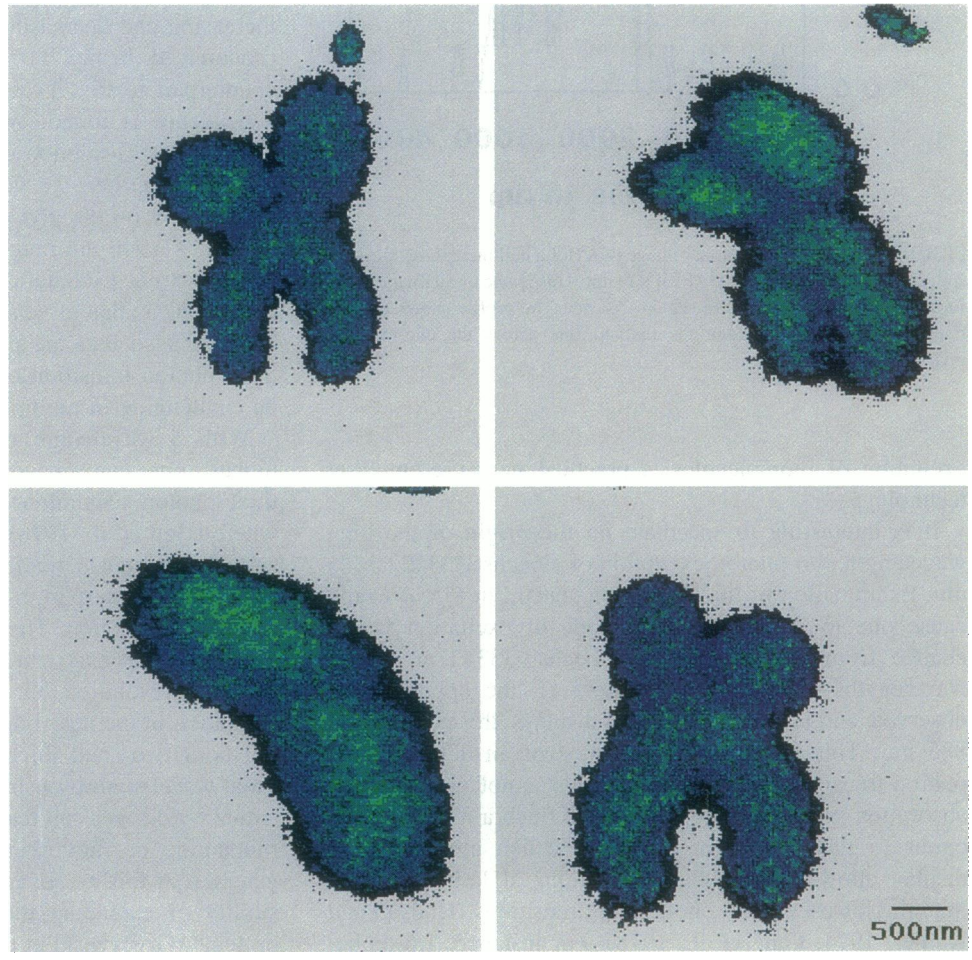

FIGURE 12 Three-dimensional images of a metaphase chromosome with $3h\nu$ excitation of DAPI at 970 nm.

addition, the doubled collection angle of the 4Pi-confocal microscope can be used. An inherent drawback of $3h\nu$ excitation microscopy is the considerably increased recording time. In most cases, however, information about the presence or absence of a dye in certain areas is sufficient. Often, with fixed samples, the recording time is of lesser importance, as in near-field optics. With fixed samples, or when information on the presence or the absence of a dye is required, $3h\nu$ excitation is a viable and useful technique in high-resolution three-dimensional fluorescence light microscopy.

This work was supported by the National Institutes of Health National Center for Research Resources, RR-08119 and RR-10416. MS and SWH acknowledge support from the European Commission.

REFERENCES

Andrews, D. L., and W. A. Ghoul. 1981. Polarization studies in multiphoton absorption spectroscopy. *J. Chem. Phys.* 75:530–538.

Barkley, M. D., and B. H. Zimm. 1979. Theory of twisting and bending of chain macromolecules: analysis of the fluorescence depolarization of DNA. *J. Chem. Phys.* 70:2991–3007.

Cable, J. R., and A. C. Albrecht. 1986. Theory of three-photon photoselection with application to the hexagonal point groups. *J. Chem. Phys.* 85:3145–3154.

Callis, P. R. 1993. On the theory of two-photon induced fluorescence anisotropy with application to indole. *J. Chem. Phys.* 99:27–37.

Chen, S-Y., and B. W. Van Der Meer. 1993. Theory of two-photon induced fluorescence anisotropy decay in membranes. *Biophys. J.* 64:1567–1575.

Denk, W. 1994. Two-photon scanning photochemical microscopy: mapping ligand-gated ion channel distributions. *Proc. Natl. Acad. Sci. USA.* 91:6629–6633.

Denk, W., K. R. Delaney, A. Gelperin, D. Kleinfeld, B. W. Strowbridge, D. W. Tank, and R. Yuste. 1994. Anatomical and functional imaging of neurons using 2-photon laser scanning microscopy. *J. Neurosci. Methods.* 54:151–152.

Denk, W., D. W. Piston, and W. W. Webb. 1995. Two-photon molecular excitation in laser scanning microscopy. *In* Handbook of Biological Confocal Microscopy, 2nd Ed. J. B. Pawley, editor. Plenum Press, New York. 445–458.

Denk, W., J. H. Strickler, and W. W. Webb. 1990. Two-photon laser scanning fluorescence microscopy. *Science.* 248:73–76.

Engelhardt, P., J. Ruokolainen, and A. Dolenc. 1994. Electron tomography of chromosomes and viruses. *CSC News.* 6:14–20.

Fang, H. L.-B., R. J. Trash, and G. E. Leroi. 1978. Observation of the low-energy ^1A_g state of diphenylhexatriene by two-photon excitation spectroscopy. *Chem. Phys. Lett.* 57:59–63.

Friedrich, D. M. 1981. Tensor patterns and polarization ratios for three-photon transitions in fluid media. *J. Chem. Phys.* 75:3258–3268.

Friedrich, D. M., and W. M. McClain. 1980. Two-photon molecular electronic spectroscopy. *Annu. Rev. Phys. Chem.* 31:559–577.

Grubb, S. G., C. E. Otis, K. S. Haber, and A. C. Albrecht. 1984. The three-photon spectrum of the $^1B_{2U} \leftarrow {}^1A_{1g}$ transition in benzene: analysis of vibronic and rotational structure. *J. Chem. Phys.* 75:5255–5265.

Gryczynski, I., and J. R. Lakowicz. 1994. Fluorescence intensity and anisotropy decays of the DNA stain HOECHST 33342 resulting from one-photon and two-photon excitation. *J. Fluoresc.* 4:331–336.

Gryczynski, I., H. Malak, and J. R. Lakowicz. 1996a. Three-photon excitation of a tryptophan derivative using a fs-Ti:sapphire laser. *Biospectroscopy.* 2:9–15.

Gryczynski, I., H. Malak, and J. R. Lakowicz. 1996b. Multi-photon excitation of the DNA stains DAPI and Hoechst. *Bioimaging.* (in press).

Gryczynski, I., H. Szmacinski, and J. R. Lakowicz. 1995. On the possibility of calcium imaging using Indo-1 with three-photon excitation. *Photochem. Photobiol.* 62:804–808.

Hanninen, P. E., and S. W. Hell. 1994. Femtosecond pulse broadening in the focal region of a two-photon microscope. *Bioimaging.* 2:117–121.

Hell, S. W., K. Bahlmann, M. Schrader, A. Soini, H. Malak, I. Gryczynski, and J. R. Lakowicz. 1996. Three-photon excitation in fluorescence microscopy. *J. Biomed. Opt.* 1:71–74.

Hell, S. W., S. Lindek, and E. H. K. Stelzer. 1994. Enhancing the axial resolution in far-field microscopy: two-photon 4Pi confocal fluorescence microscopy. *J. Mod. Opt.* 41:675–681.

Hell, S. W., M. Schrader, P. E. Hanninen, and E. Soini. 1995. Resolving fluorescence beads at 100–200 nm axial distance with a two-photon 4Pi-microscope operating in the near infrared. *Opt. Commun.* 120: 129–133.

Hudson, B., and B. Kohler. 1974. Linear polyene electronic structure and spectroscopy. *Annu. Rev. Phys. Chem.* 25:437–460.

Laczko, G., J. R. Lakowicz, I. Gryczynski, Z. Gryczynski, and H. Malak. 1990. A 10 GHz frequency-domain fluorometer. *Rev. Sci. Instrum.* 61:2331–2337.

Lakowicz, J. R., H. Cherek, J. Kuśba, I. Gryczynski, and M. L. Johnson. 1993. Review of fluorescence anisotropy decay analysis by frequency-domain fluorescence spectroscopy. *J. Fluoresc.* 3:103–116.

Lakowicz, J. R., and I. Gryczynski. 1991. Frequency-domain fluorescence spectroscopy. *In* Topics in Fluorescence Spectroscopy, Vol. 1: Techniques. J. R. Lakowicz, editor. Plenum Press, New York. 293–355.

Lakowicz, J. R., and I. Gryczyński. 1992. Fluorescence intensity and anisotropy decay of the 4′,6-diamidino-2-phenylindole-DNA complex resulting from one-photon and two-photon excitation. *J. Fluoresc.* 2:117–122.

Lakowicz, J. R., and I. Gryczynski. 1993. Tryptophan fluorescence intensity and anisotropy decays of human serum albumin resulting from one-photon and two-photon excitation. *Biophys. Chem.* 45:1–6.

Lakowicz, J. R., I. Gryczynski, E. Danielsen, and J. K. Frisoli. 1992a. Unexpected anisotropy spectra of indole and *N*-acetyl-L-tryptophanamide observed for two-photon excitation of fluorescence. *Chem. Phys. Lett.* 194:282–287.

Lakowicz, J. R., I. Gryczynski, J. Kuśba, and E. Danielsen. 1992b. Two photon-induced fluorescence intensity and anisotropy decays of diphenylhexatriene in solvents and lipid bilayers. *J. Fluoresc.* 2:247–258.

Lakowicz, J. R., B. Kierdaszuk, P. R. Callis, H. Malak, and I. Gryczynski. 1994a. Fluorescence anisotropy of tyrosine using one- and two-photon excitation. *Biophys. Chem.* 56:263–271.

Lakowicz, J. R., H. Szmacinski, K. Nowaczyk, W. J. Lederer, and M. L. Johnson. 1994b. Fluorescence lifetime imaging of intracellular calcium in COS cells using Quin-2. *Cell Calcium.* 15:7–27.

Malak, H., I. Gryczynski, J. D. Dattelbaum, and J. R. Lakowicz. 1996. Three-photon induced fluorescence of diphenylexatriene in solvents and lipid bilayers. *J. Fluoresc.* (in press).

Millar, D. P., R. J. Robbins, and A. H. Zewail. 1982. Torsion and bending of nucleic acids studied by subnanosecond time-resolved fluorescence depolarization of intercalated dyes. *J. Chem. Phys.* 76:2080–2094.

Pradere, F., J. Hanus, and M. Schott. 1966. Optique moleculaire. *C. R. Acad. Sci. Paris.* 263:372–375.

Rehms, A. R., and P. R. Callis. 1993. Two-photon fluorescence excitation spectra of aromatic amino acids. *Chem. Phys. Lett.* 208:276–282.

Sammeth, D. M., S. Yan, L. H. Spangler, and P. R. Callis. 1990. Two-photon fluorescence excitation spectra of indole in vapor and jet: ^1L_a states. *J. Phys. Chem.* 94:7340–7342.

Schurr, J. M., B. S. Fujimoto, P. Wu, and L. Song. 1992. Fluorescence studies of nucleic acids: dynamics, rigidities, and structures. *In* Topics in Fluorescence Spectroscopy, Vol. 3: Biochemical Applications. J. R. Lakowicz, editor. Plenum Press, New York. 137–229.

Singh, S., and L. T. Bradley. 1964. Three-photon absorption in naphthalene crystals by laser excitation. *Phys. Rev. Lett.* 12:612–615.

Spectra Physics Lasers, Inc. 1995. Tsunami improves two-photon fluorescence images. *Laser Forefront.* 4:1–4.

Stelzer, E. H. K., S. Hell, S. Lmdek, R. Stricker, R. Pick, C. Storz, G. Ritter, and N. Salmon. 1994. Nonlinear absorption extends confocal

fluorescence microscopy into the ultra-violet regime and confines the illumination volume. *Opt. Commun.* 104:223–228.

Svoboda, K., and S. M. Block. 1994. Biological applications of optical forces. *Annu. Rev. Biophys. Biomol. Struct.* 23:247–285.

Szmacinski, H., I. Gryczynski, and J. R. Lakowicz. 1996. Three-photon induced fluorescence of the calcium probe indo-1. *Biophys. J.* 70: 547–555.

Wan, C., and C. K. Johnson. 1994a. Time-resolved anisotropic two-photon spectroscopy. *Chem. Phys.* 179:513–531.

Wan, C., and C. K. Johnson. 1994b. Time-resolved two-photon induced anisotropy decay: the rotational diffusion regime. *J. Chem. Phys.* 101: 10283–10291.

Webb, W. W. 1990. Two photon excitation in laser scanning fluorescence microscopy. *MICRO 90 London.* 13:445–450.

Webb, W. W. 1996. Three-photon excited fluorescence and applications in nonlinear laser scanning microscopy. *Biophys. J.* 70:A429.

Wirth, M. J., A. Koskelo, and M. J. Sanders. 1981. Molecular symmetry and two-photon spectroscopy. *Appl. Spectrosc.* 35:14–21.

Wokosin, D. L., V. E. Centonze, J. G. White, S. N. Hird, S. Sepsenwol, G. P. A. Malcom, G. T. Maker, and A. I. Ferguson. 1996. Multiple excitation imaging with an all-solid-state laser. Proceedings of optical diagnostics of living cells and biofluids. The International Society for Optical Engineering (*SPIE*). 2678:38–49.